Desalination and Water Treatment
www.deswater.com
doi: 10.1080/19443994.2015.1119747

57 (2016) 21444–21454
September

Taylor & Francis
Taylor & Francis Group

Adsorption of ammonia from wastewater using low-cost bentonite/chitosan beads

M. Gaouar Yadi[a,*], B. Benguella[b], N. Gaouar-Benyelles[a], K. Tizaoui[b]

[a]*Laboratory of Ecology and Management of Naturals Ecosystems, Biology and Environment Department, Abu Bakr Belkaid University, Imama, Tlemcen, Algeria, Tel. +97466550179; email: gaouar_manel@yahoo.fr (M. Gaouar Yadi), Tel. +213 560037225; email: gaouarn@yahoo.fr (N. Gaouar-Benyelles)*
[b]*Laboratory of Inorganic Chemistry and Environment, Faculty of Sciences, Chemistry Department, University of Tlemcen, 13000, Algeria, Tel. +213 551677376; emails: belkacem_71@yahoo.fr (B. Benguella), khadidja.tizaoui@hotmail.fr (K. Tizaoui)*

Received 26 April 2015; Accepted 24 October 2015

ABSTRACT

The inexpensive and eco-friendly biosorbents bentonite–chitosan and bentonite–chitin coagulants have been successfully utilized for their ammonia removal efficiency. Bentonite was prepared using the flocculation–coagulation method. A bentonite–chitosan composite achieved its maximum ammonia removal capacity of 11.6 mg/g, whereas natural bentonite and bentonite–chitin coagulants showed ammonia adsorption capacity of 0.75 and1.04 mg/g, respectively. The optimum pH value was observed at pH 6, while the effect of temperature, contact time, and initial concentrations on the adsorption capacity of the adsorbent has also been investigated. Infrared spectrometry (FTIR) was used to characterize the adsorbent. Freundlich isotherm best explained the experimental data over a Langmuir model for all applied adsorbents. The ammonia adsorption followed a pseudo-second-order kinetic model. Ammonia surface adsorption followed an endothermic process, encouraged by higher temperature values.

Keywords: Bentonite; Chitosan; Chitin; Ammonia; Adsorption kinetics

1. Introduction

Adsorption technology has been widely studied as an efficient method for denitrification from wastewater [1]. Recent research work has been devoted to develop low-cost adsorbents to improve cost-effectiveness of denitrification using this technology. For example, chitin composite [2] modified chitosan beads [3], synthetic apatites [4], and bentonite clay [5] have been demonstrated as effective adsorbents for ammonia removal. Subsequently, the adsorbent can be regenerated or must be kept in a dry place without direct contact with the environment [6,7].

Bentonite is a hydrous aluminum silicate, a common group of clay minerals reported as low-cost materials. However, the low adsorption capacity of bentonite is the major problem for its possible application for denitrification, therefore, it is important to modify raw bentonite to determine whether its adsorption rate can be improved to suit a potential application for ammonia removal.

Chitosan, also named poly(β-1,4)-2-amino-2-deoxy-D-glucopyranose, is prepared from chitin by partial or total deacetylation. Chitosan is a biopolymer that has

*Corresponding author.

been cited as an excellent material for coagulation–flocculation processes. However, raw chitin, and its deacetylyzed version chitosan, used alone are unstable, and the adsorption capacity of each is minimal [8]. Like bentonite, it is necessary to modify chitin and chitosan physically or chemically to determine whether adsorption rates can be improved to a point they become practical to use for denitrification.

The present study investigated the potential to form inexpensive and efficient adsorbents from the bentonite, chitosan, and chitin. Adsorption equilibrium experiments were used to investigate the adsorption behavior of combinations of bentonite–chitosan and bentonite–chitin. The effects of various parameters such as bentonite dosage, pH, temperature, initial ammonia concentration, and contact time on adsorption capacity of bentonite–chitosan and bentonite–chitin were studied. A first-order kinetic model and pseudo-second-order kinetic model were employed to understand the adsorption process. Freundlich and Langmuir models were applied to determine the physiochemical properties of the adsorbents. FTIR analysis was also undertaken to characterize the bentonite/chitosan and bentonite/chitin combinations before and after ammonia adsorption.

2. Materials and methods

2.1. Materials

All reagents are of analytical grade. Bentonite used in the study is extracted from the deposit at Hammam-Boughrara Maghnia (Tlemcen). It was provided by Entreprise Nationale BENTAL of Maghnia (Tlemcen) as a finely divided powder (about 54% of the grains have a diameter less than 2 μm). The specific surface area measured by nitrogen adsorption at 77 K for bentonite is 23 m^2/g. The chemical composition results of bentonite revealed a high content of SiO_2 trend aluminum [9].

Chitin and chitosan were provided by the laboratory of the Inorganic Chemistry and Environment, at the Department of Chemistry, Faculty of Sciences, University of Tlemcen, in Algeria.

2.2. Adsorption experiments

Adsorption experiments are carried out with 500 mL of wastewater solution at a constant speed of 200 rpm at 25°C for 10 min.

Adsorption tests are initially conducted on each of the materials alone.

Experiments are then conducted on blends of bentonite–chitosan, and bentonite–chitin. First, 7.5 g of bentonite adsorbent is added to the wastewater solution. Then, a 0.3 g concentration of chitosan powder or chitin is added to the initial solution and stirred for three minutes (coagulation). The stirring speed is then reduced to 40 rpm for 20 min (flocculation) [10]. In this study, all the adsorption experiments are conducted in triplicate. The initial average ammonia concentration is shown in Table 1 along with other tested parameters. Ammonia adsorption is studied under different conditions including pH, temperature, contact time, and initial concentration. After reaching adsorption equilibrium, the ammonia concentration is measured using a spectrophotometer (Hach DR 2800).

The amount of adsorbed ammonia was calculated using the following equation:

$$q_t = (C_0 - C_e)V/m \quad (1)$$

where q_t is the amount of adsorbed pollutant (mg per gram of bentonite), C_0 and C_e are, respectively, the initial and instantaneous concentrations of pollutant (mg/L), V is the volume of solution (L), and m the mass of the adsorbent used (g).

2.3. FTIR analysis

The films are dried at 60°C overnight before measurement. The chemical structure of the pure material films and blend films are investigated using FTIR measurement. FTIR measurements are performed using KBr pelleted samples with a Perkins Elmer 200 FTIR spectrophotometer with a resolution of 4 cm^{-1} in the range of 400–4,000 cm^{-1}.

3. Results and discussion

3.1. Kinetics study

In order to optimize the dosage and reduce the ammonia concentration in the aqueous solution, raw chitin and raw chitosan were used to adsorb ammonia under identical experimental conditions. Then both chitosan and chitin were mixed with 7.5 g bentonite to test binary adsorption capacity.

Table 1
Influent average parameters

Parameters	
NH-3 (mg/l)	26.4
TP (mg/l)	5.79
Turbidity (NTU)	88.9
BOD_5 (mg/l)	197

The results in Fig. 1 show that the maximum adsorption capacity of bentonite, chitin, and chitosan were 1.29, 3.2, and 7.6 mg/g, respectively. The bentonite–chitosan coagulant achieved its maximum capacity at 11.6 mg/g, and bentonite/chitin showed 1.04 mg/g maximum adsorption. Similar findings have been confirmed by Barrow [11,12], who has demonstrated that by adding bentonite to chitin or chitosan to the coagulation/flocculation process the coagulant positively influenced pollutant removal.

3.2. Effect of pH on adsorption

The adsorption data obtained for the effect of different pH values of 4, 6, and 8 on ammonia removal are shown in Figs. 2a–2e.

The ammonia adsorption efficiency was calculated using the following equation:

$$\eta = [C_0 - C_e/C_0] \times 100 \quad (2)$$

where C_0 and C_e are the initial and final concentrations, respectively.

Fig. 2a reflects that ammonia has been better adsorbed at pH 4 and pH 6 on bentonite, with a removal efficiency of 100%.

At pH 8, ammonia removal efficiency reached 57 and 70%, respectively, on chitin as shown in Fig. 2c, and bentonite–chitin (Fig. 2e).

However, unlike the Barrow findings [11,12], wherein the removal percentage of bentonite/chitosan composite was at its maximum for ammonia, it acted reversely and decreased significantly to 31% for bentonite–chitosan at pH 4 and 6 (Fig. 2d) and 30% for bentonite–chitin, while it reached 63.60% of removal on chitosan at pH 8 (Fig. 2b).

Zhang et al. [13] showed the same finding with fluoride adsorption capacity on bentonite/chitosan beads, wherein the adsorption capacity declined with the increase in pH value. The Zhang results also reflected that the acidic pH could allow more adsorption sites on bentonite/chitosan beads for fluoride removal but that alkaline pH was undesirable for adsorption process for fluoride.

3.3. Pseudo-second-order kinetic model

The effect of contact time (30, 60, 120, and 180 min) on adsorption of ammonia using bentonite–chitosan was observed in Fig. 3. According to Azhar et al. [14], a higher removal percentage is achieved at the beginning of the adsorption. The adsorption percentage decreases sharply as the agitation period increases. The same observation was been made by Erdem et al. [15].

The uptake of ammonia reached equilibrium within 10 min with 100% of removal onto bentonite, while on bentonite–chitosan, the uptake reached equilibrium within 30 min, with a removal rate of 60%.

Pseudo-second-order kinetic assumes that chemisorption controls the adsorption rate [16]. In order to achieve the adsorption behavior through the whole range of process, a pseudo-second-order kinetic

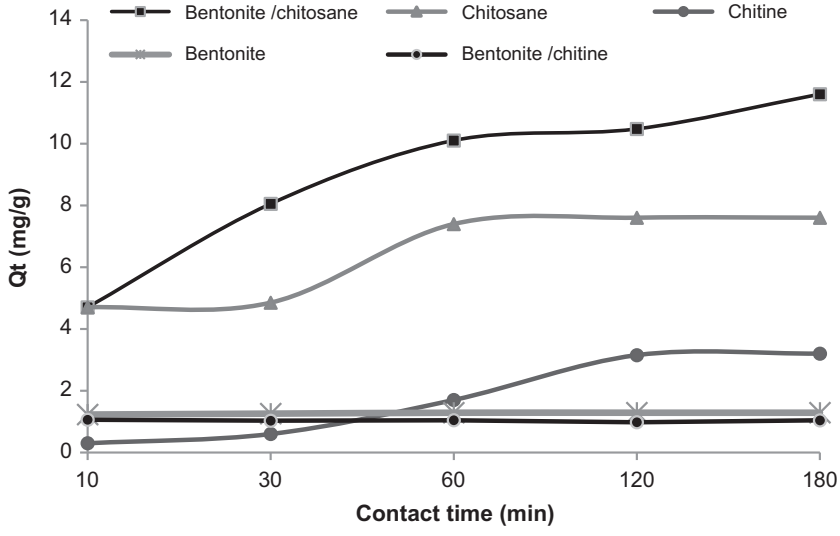

Fig. 1. Adsorption kinetics of different adsorbents on ammonia (pH 8, initial concentration 26.4 mg/L, contact time 180 min, and agitation speed 200 rpm).

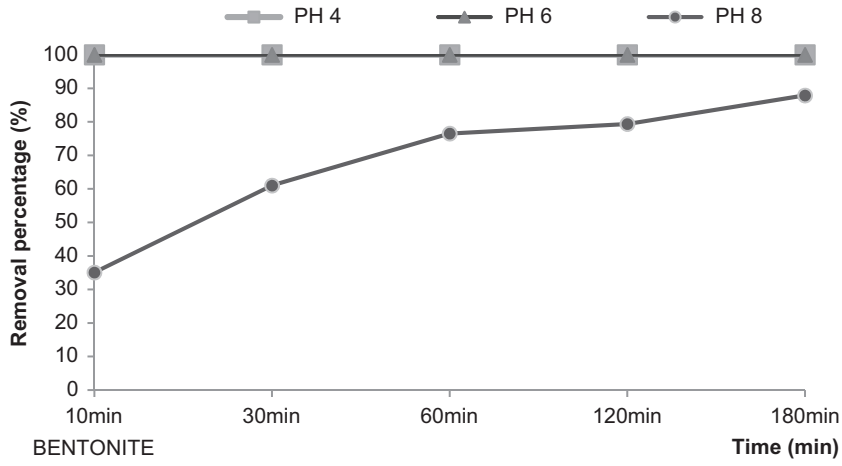

Fig. 2a. Effect of pH on ammonia removal on bentonite (initial concentration 49.7 mg/L, contact time 180 min, and agitation speed 200 rpm).

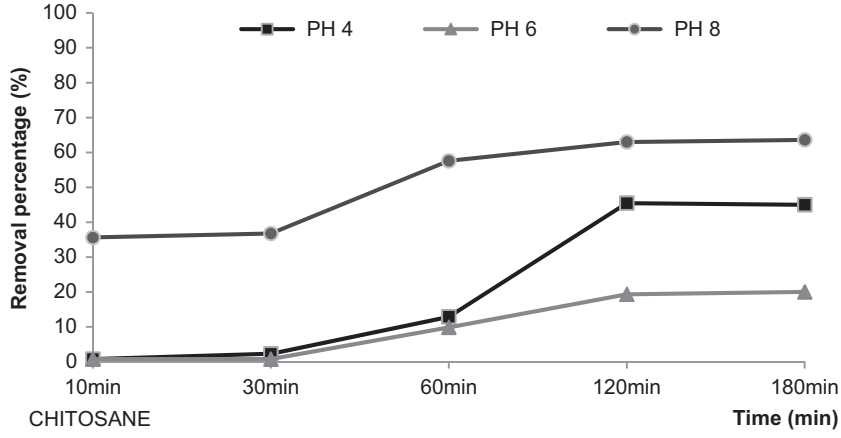

Fig. 2b. Effect of pH on ammonia removal on chitosan (initial concentration 49.7 mg/L, contact time 180 min, and agitation speed 200 rpm).

model was used to analyze the adsorption data. The linear form of pseudo-second-order kinetic equation can be expressed as:

$$\frac{t}{q_t} = \frac{1}{k_2 q_e^2} + \frac{1}{q_e} t \tag{3}$$

where t is the contact time (min), q_t and q_e are the amounts of ammonia adsorbed (mg/g) at arbitrary time t and at equilibrium, respectively. k_2 is the adsorption rate constant (g/mg min).

The plots for the pseudo-second-order kinetic model of adsorbent are shown in Fig. 3 for ammonia adsorption. The correlation coefficients (R^2) value was larger than 0.99, which suggested the adsorption followed the pseudo-second-order kinetic model, and from the values of q_e shown in Table 2, it was noted that the values calculated using the pseudo-second-order model were the closest to those achieved experimentally.

3.4. Thermodynamics of ammonia adsorption

In general, adsorption is accompanied by a thermal process that can either be exothermic ($\Delta H > 0$) or endothermic ($\Delta H < 0$). The measurement of ΔH enthalpy is the main criterion that differentiates chemisorption from physisorption.

The enthalpy of adsorption is explained using the following relationships:

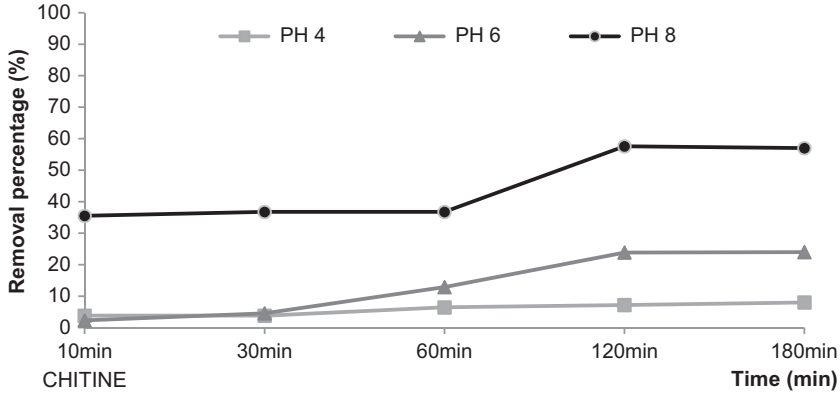

Fig. 2c. Effect of pH on ammonia removal on chitin (initial concentration 49.7 mg/L, contact time 180 min, and agitation speed 200 rpm).

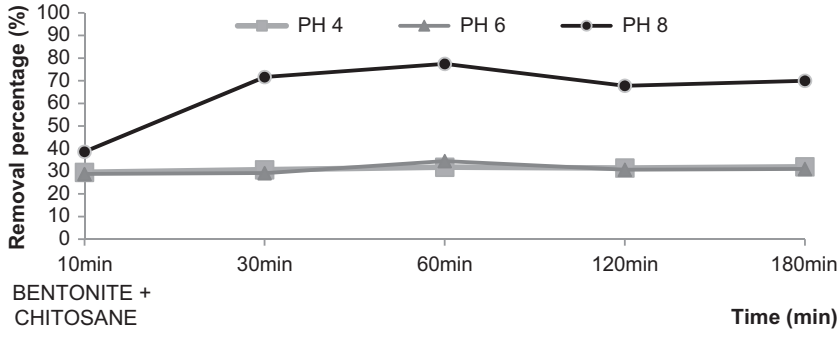

Fig. 2d. Effect of pH on ammonia removal on bentonite–chitosan (initial concentration 49.7 mg/L, contact time 180 min, and agitation speed 200 rpm).

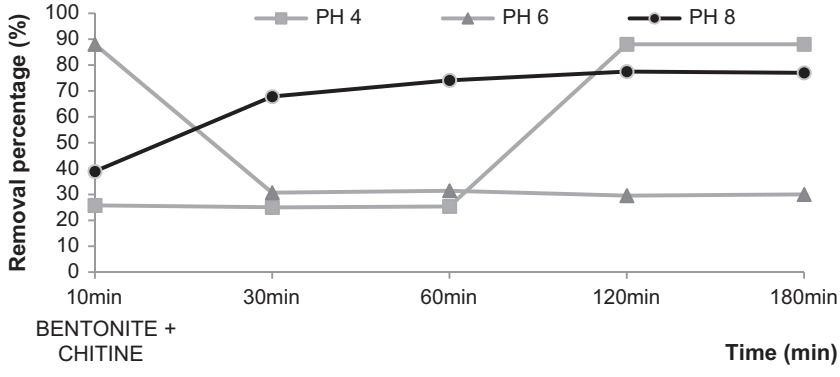

Fig. 2e. Effect of pH on ammonia removal on bentonite–chitin (initial concentration 49.7 mg/L, contact time180 min, and agitation speed 200 rpm).

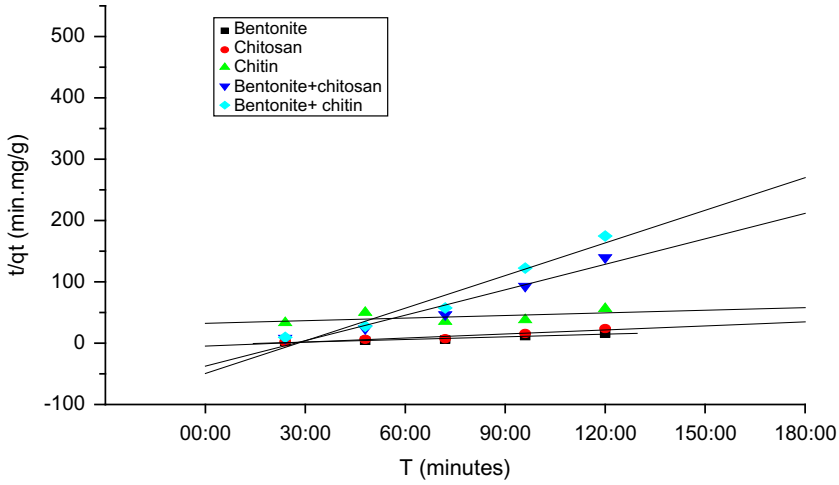

Fig. 3. Pseudo-second-order kinetic plot for ammonia adsorption.

Table 2
Comparison between calculated and tested data of adsorption of various pollutants on various beads

Adsorbent	$q_{e,exp}$ (mg/g)	$q_{e,cal}$ (mg/g) pseudo-second-order	$q_{e,cal}$ (mg/g) second-order	R^2	STDV	P
Bentonite	11.6	12.46	14.53	0.951	1.42	0.004
Chitosan	7.6	8.087	52.3	0.924	2.74	0.008
Chitin	3.2	7.87	5.39	0.827	9.75	0.35
Bentonite + chitosan	1.29	1.294	1.88	0.952	13.54	0.004
Bentonite + chitin	1.04	1.012	0.327	0.952	17.31	0.004

$$\ln K_c = \frac{\Delta S}{R} - \frac{\Delta H}{RT} \quad (4)$$

with

$$K_c = \frac{C_e}{(C_0 - C_e)} \quad (5)$$

where K_c is the equilibrium constant, ΔH enthalpy (J/mol), ΔS entropy (J/mol/K), T absolute temperature (K), C_0 is initial concentration of adsorbate, C_e the equilibrium concentration of adsorbate, and R the gas constant (8.314 J/mol K).

The thermodynamic parameters ΔH and ΔS of ammonia on the different supports are determined graphically by plotting $\ln K_c$ vs. the inverse of the environmental temperature in Kelvin degrees.

Fig. 4 shows straight lines with good correlation coefficients, which enables calculating ΔH and ΔS for adsorption of ammonia using different supports.

The positive values of ΔH in Table 3 confirmed that the adsorption of ammonia is an endothermic process. Low values of this enthalpy (>40 kJ/mol) showed that this was a chemical adsorption. The positive values of entropy showed that ammonia adsorption is followed by an increased medium disorder.

As seen in Fig. 5, the adsorption capacity of adsorbent declined with the rise in temperature, which is perhaps because the high temperature resulted in the instability of the adsorbents in general.

3.5. Freundlich isotherm model

The Freundlich adsorption isotherm is an empirical equation used to describe a heterogeneous system. The Freundlich adsorption isotherm from aqueous solution is represented in linear form as follows:

$$\ln q_e = \ln K_F + \frac{\ln C_e}{n} \quad (6)$$

where K_F and n are the constants of Freundlich isotherm indicating adsorption capacity and adsorption intensity, respectively. The Freundlich constants, i.e. $1/n$ and K_F were calculated from the slope and intercept of Freundlich plots of $\ln q_e$ vs. $\ln C_e$. The

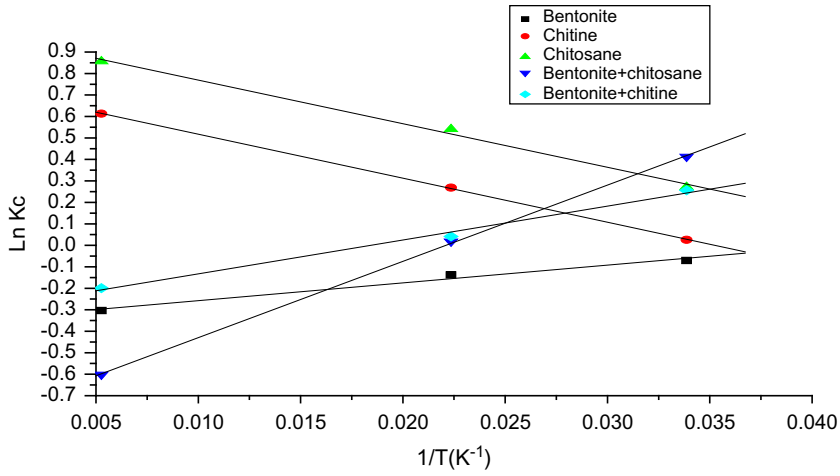

Fig. 4. Enthalpy determination of ammonia entropy by solid support.

Table 3
Thermodynamics parameters

	ΔH (kJ/mol)	ΔS (kJ/mol)	R^2	N	STDV	P
Bentonite	43.868	1.3121×10^4	0.983	3	0.021	0.08
Chitin	40.627	1.1372×10^4	0.99	3	0.005	0.008
Chitosan	46.696	1.2995×10^4	0.995	3	0.027	0.042
Bentonite + Chitin	25.760	8.8971×10^3	0.993	3	0.001	0.009
Bentonite + Chitosan	79.041	2.3357×10^4	0.999	3	0.025	0.05

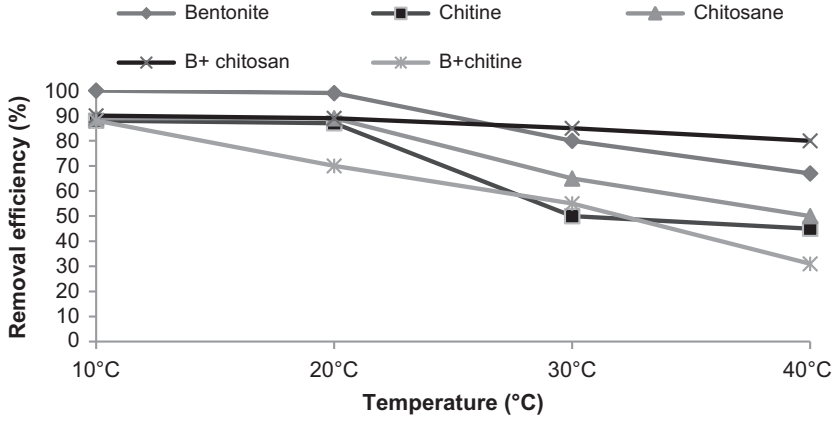

Fig. 5. Effect of temperature on adsorption of ammonia by different sorbents (pH 8, initial concentration 35 mg/L, contact time 120 min, and agitation speed 200 rpm).

correlation coefficient and other parameters obtained for the adsorbent are shown in Table 4.

From Table 4, we can deduce that the obtained Freundlich constant (as shown in Table 3) represents adsorption intensity; n was less than 1 ($n < 1$) for all types of adsorbent media, while $n > 1$ showed good adsorption, that is, it demonstrates that good adsorption was occurring throughout the concentration range [17]. Therefore, the results indicate that the equilibrium data was not fitted well with the Freundlich isotherm model compared with the Langmuir isotherm model.

Table 4
Langmuir and Freundlich isotherm constant for adsorption of ammonia onto different adsorbents

	Freundlich			Langmuir		
Support	n	K_F (mg/g)	R^2	b (L/mg)	Q_m (mg/g)	R^2
Bentonite	1.51	8.98	0.9802	0.17	125	0.9792
Chitosan	1.56	5.87	0.9941	0.30	111	0.9911
Chitin	1.70	4.19	0.9973	0.46	83	0.9599
Bentonite + Chitosan	0.43	1.96	0.987	0.05	15.90	0.971
Bentonite + Chitin	0.42	2.05	0.986	0.05	16.16	0.973

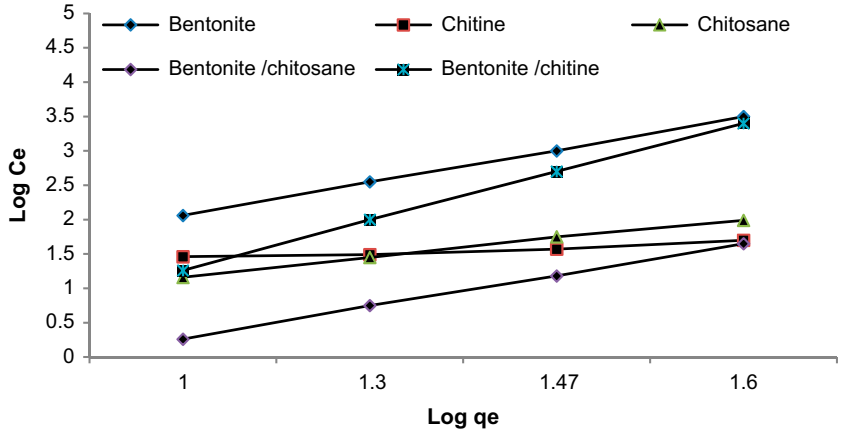

Fig. 6. Fitting curve of Freundlich adsorption isotherm of adsorbent.

Table 5
Infrared data of raw and modified bentonite

Bands assignments	Bentonite	Bentonite–chitosan	Bentonite–chitin
ν_{OH} stretching (H_2O)	3,800; 3,200	3,630; 3,422	3,200; 3,800
ν_{OH} deformation (H_2O)	1,600	1,644	600
ν_{SiO} stretching vibration	1,020	1,036	1,200; 800
δ_{Al-O-H}	900	880	900
δ^{VI}_{Si-O-M}	550	522	
Quartz	1,034; 915; 798; 694	795	
Calcite	1,390		

The fitting curve of Freundlich adsorption isotherm for ammonia adsorption is shown in Fig. 6. The effect of temperature and initial ammonia concentration on adsorption capacity of different adsorbents were studied. It was observed that the adsorption capacity had increased up to 1.7 mg/g at 20°C for bentonite with initial ammonia concentration of 15 mg/L, and increased to 2.25 mg/g at 20°C with initial ammonia concentration of 15 mg/L for bentonite–chitosan composite, and the capacity was 0.46 mg/g for bentonite–chitin at 30°C with initial ammonia concentration of 15 mg/L. The correlation coefficients (R^2) values showed that the adsorption data could be well described by Freundlich isotherm model, which suggested that all beads were heterogeneous adsorbents.

3.6. Characterization

The FTIR spectra of bentonite, chitosan, and chitin beads before and after intercalation are compared in Table 5. Pure bentonite clay shows characteristic

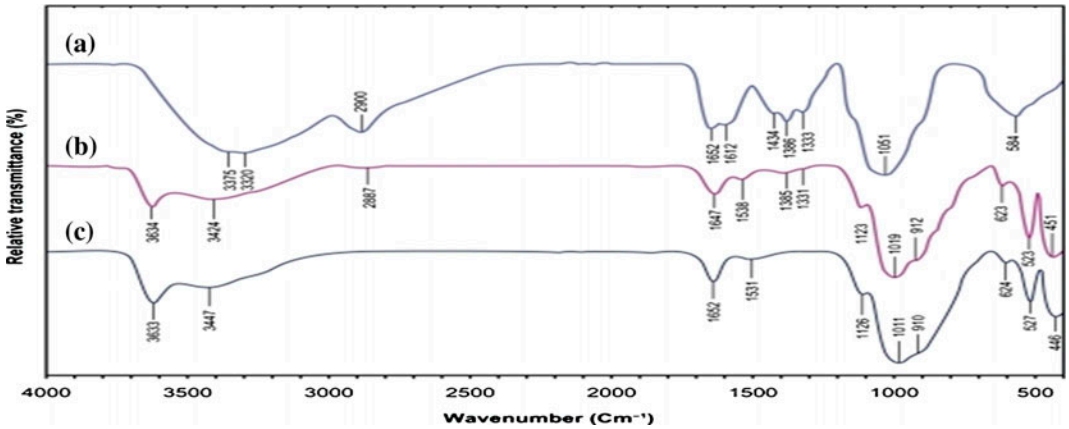

Fig. 7a. Infrared spectra for (a) chitosan, (b) bentonite-chitosan, and (c) bentonite.

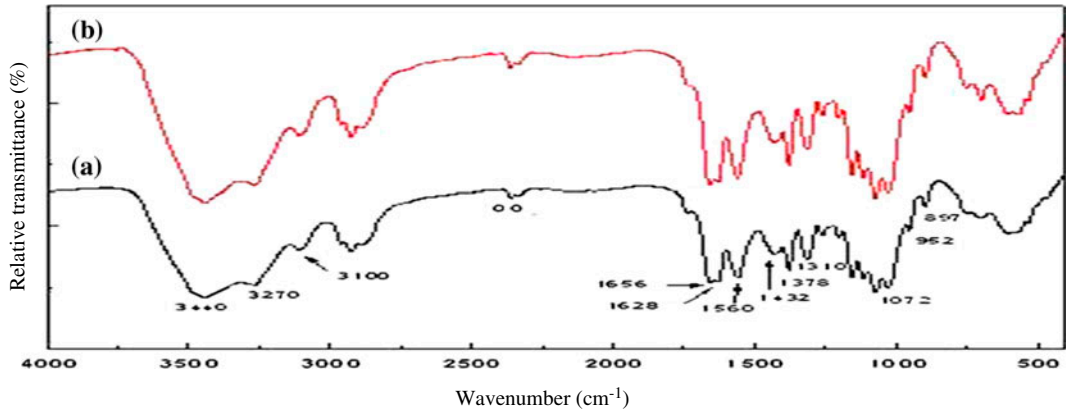

Fig. 7b. Infrared spectra for (a) chitin and (b) bentonite-chitin.

Table 6
Infrared data of chitin

Peak assignment	Wave number (cm^{-1})
ν_{OH} stretching (H_2O)	3,450
(CH_2–CH_3) stretching	2,940; 2,980
C–H bending vibrations in the group CH_3	1,375
C–H bending vibrations in the group CH_2	1,440; 1,480
C=O (Amide I) valence vibration	1,650
N–H bending vibrations in (Amide II)	1,550
Valence vibration on C–N	1,320
Valence vibration on C–O–C	1,080; 1,160
Valence vibration on C–OH	1,030

vibration bands were located between 3,200 and 3,800 cm^{-1} (OH stretching from lattice hydroxyl), 1,020 cm^{-1} (Si–O stretching), and 900 cm^{-1} (Al–O stretching).

Natural chitin showed characteristic vibration bands locating the broad band at the region of 3,450 cm^{-1} which was the overlapping peak of $–NH_2$ and –OH stretching vibrations for beads, between

Table 7
FT-IR analysis of chitosan

Peak assignment	Wave number (cm^{-1})
N–H and O–H stretching	3,480
C–H stretching vibrations in the group CH_2 or CH_3	2,890; 2,923
C–H bending vibrations in the group CH_3	1,381
C–H bending vibrations in the group CH_2	1,421; 1,470
C=O (Amide I) valence vibration	1,637
N–H bending vibrations in (Amide II)	1,601
Valence vibration on C–N	1,310
Valence vibration on C–O–C	1,091; 1,154
Valence vibration on C–OH	1,020

2,940 and 2,980 cm^{-1} (–CH_3 and –CH_2 stretching vibrations, respectively), 1,375 cm^{-1} (which was the characteristic of the bending vibration of –CH on –CH_3 stretching vibrations), between 1,440 and 1,480 cm^{-1} (the characteristic of the bending vibration of -CH on -CH_2 stretching vibrations), and between 1,080 and 1,160 cm^{-1} (was the characteristic of the C–O–C stretching vibrations).

On the other hand, the bentonite–chitin FTIR spectra in Fig. 7a and Table 6 showed characteristic vibration bands located between 3,200 and 3,800 cm^{-1}.

As for chitosan, the FTIR spectra in Fig. 7b and Table 7 shows the band located between 2,923 and 2,890 cm^{-1} (–CH_3 and –CH_2 stretching vibrations, respectively). At 1,633 cm^{-1}, the absorbance peak of symmetric stretching of –C–N appeared, suggesting that –OH on C3 reacted with bentonite to form chitosan beads [18].

Furthermore, bentonite–chitosan FTIR spectra in Fig. 7b was characterized by the broad band at the region of 3,450 cm^{-1} which was the overlapping peak of –NH_2 and –OH stretching vibrations for beads [19]. The FTIR spectra confirmed the successful synthesis of bentonite–chitosan and bentonite–chitin beads.

4. Conclusions

(1) The study of the adsorption of ammonia has been successful and showed that bentonite–chitosan beads are better adsorbents compared to bentonite–chitin bead and bentonite alone, due to the high surface area and high porosity of the beads, and the low cost and abundance of the raw materials.
(2) A bentonite–chitosan composite adsorbent possesses a higher CEC value compared to the other sorbents. Based on the batch adsorption study, the removal of ammonia was well-fitted with the Langmuir isotherm model. This shows that the adsorption process was by monolayer adsorption due to specific bonding between adsorbate and the surface of adsorbent. This was also supported by the results of kinetic study for ammonia removal, which was obtained following the pseudo-second-order model. This model, used to explain the probability of overall adsorption properties, was suited to the chemical adsorption mechanism.
(3) The optimum dosage of bentonite–chitosan was 0.3/7.5 g with adsorption capacity of 12.46 mg/g. The optimum pH value for ammonia adsorption was pH 6. The adsorption capacity of adsorbent was at its maximum efficiency of 100% after 10 min of contact time onto natural bentonite.
(4) Ammonia surface adsorption had been found to be an endothermic process and is favored by higher temperatures.

References

[1] W. Ma, F.-Q. Ya, M. Han, R. Wang, Characteristics of equilibrium, kinetics studies for adsorption of fluoride on magnetic-chitosan particle, J. Hazard. Mater. 143 (2007) 296–302.
[2] C. Sairam Sundaram, N. Viswanathan, S. Meenakshi, Fluoride sorption by nano-hydroxyapatite/chitin composite, J. Hazard. Mater. 172 (2009) 147–151.
[3] D. Thakre, S. Jagtap, N. Sakhare, N. Labhsetwar, S. Meshram, S. Rayalu, Chitosan-based mesoporous Ti–Al binary metal oxide-supported beads for defluoridation of water, Chem. Eng. J. 158 (2010) 315–324.
[4] A. Yehia, K. Ezzat, Fluoride ion uptake by synthetic apatites, Adsorpt. Sci. Technol. 27 (2009) 337–347.
[5] S.P. Kamble, P. Dixit, S.S. Rayalu, N.K. Labhsetwar, Defluoridation of drinking water using chemically-modified bentonite clay, Desalination 249 (2009) 687–693.
[6] E. Bazrafshan, A. Zarei, H. Nadi, M.A. Zazouli, Adsorptive removal of methyl orange and reactive red 198 by moringa peregrina ash, Indian J. Chem. Technol. 21 (2014) 105–113.

[7] B. Royer, NF. Cardoso, EC. Lima, VSO. Ruiz, TR. Macedo, C. Airoldi, Organofunctionalized kenyaite for dye removal from aqueous solution, J. Colloid Interface Sci. 336 (2009) 398–405.
[8] P. Miretzky, A.F. Cirelli, Fluoride removal from water by chitosan derivatives and composites: A review, J. Fluorine Chem. 132 (2011) 231–240.
[9] B. Benguella, A. Yacouta-Nour, Elimination des colorants acides en solution aqueuse par la bentonite et le kaolin (Acidic dye removal in aquous solution using bentonite and Kaolin), Comptes Rendus Chimie 12 (2009) 762.
[10] M. Ferhat, Co-adsorption des métaux lourds sur la bentonite modifiée en présence de floculants minéraux et biologiques (Heavy metals co-adsorption on modified bentonite using mineral and biologic floculants), Masters thesis, 2012, p. 140.
[11] N.J. Barrow, A discussion of the methods for measuring the rate of reaction between soil and phosphate, Fertilizer Res. 4 (1983) 51–61.
[12] N.J.A. Barrow, A mechanistic model for describing the sorption and desorption of phosphate by soil, J. Soil Sci. 34 (1983) 733–750.
[13] Y. Zhang, W. Dongfeng, L. Bingjie, G. Xiang, X. Wei, L. Peng, X. Ying, Adsorption of fluoride from aqueous solution using low-cost bentonite/chitosan beads, Am. J. Anal. Chem. 04 (2013) 48–53.
[14] S. Azhar, A.G. Liew, D. Suhardy, K.F. Hafiz, M.D.I. Hatim, Dye removal from aqueous solution by using adsorption on treated sugarcane bagasse, Am. J. Appl. Sci. 2 (2005) 1499–1503.
[15] E. Erdem, G. Çölgeçen, R. Donat, The removal of textile dyes by diatomite earth, J. Colloid Interface Sci. 282 (2005) 314–319.
[16] N.J. Barrow, T.C. Shaw, The slow reactions between soil and anions, Soil Sci. 119 (1975) 167–177.
[17] M.S. Chiou, H.Y. Li, Adsorption behavior of reactive dye in aqueous solution on chemical cross-linked chitosan beads, Chemosphere 50(8) (2003) 1095–1105.
[18] B. Liu, D. Wang, X. Gao, L. Zhang, Y. Xu, Y. Li, Removal of arsenic from laminaria japonica aresch juice using As(III)-imprinted chitosan resin, Eur. Food Res. Technol. 232 (2011) 911–917.
[19] A.S. Özcan, A. Özcan, Adsorption of acid dyes from aqueous solutions onto acid-activated bentonite, J Colloid Interface Sci. 276 (2004) 39–46.